Supplementary Information

New Schiff base copper(II) and nickel(II) complexes for biomedical applications with reference to SARS-CoV-2 and HIV virus

Aprajita & Mukesh Choudhary*

Department of Chemistry, National Institute of Technology Patna, Patna -800 005, Bihar, India
*E-mail: mukesh@nitp.ac.in

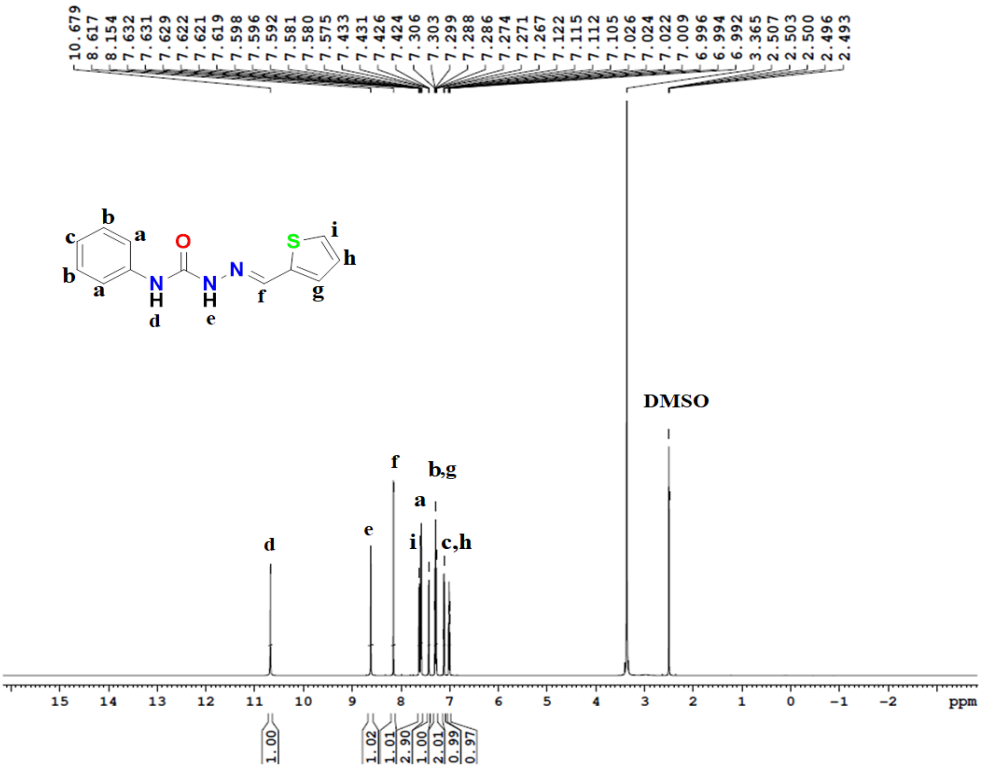

Fig. S1— ^{1}H-NMR of synthesized Schiff base Ligand **L^{1}H**

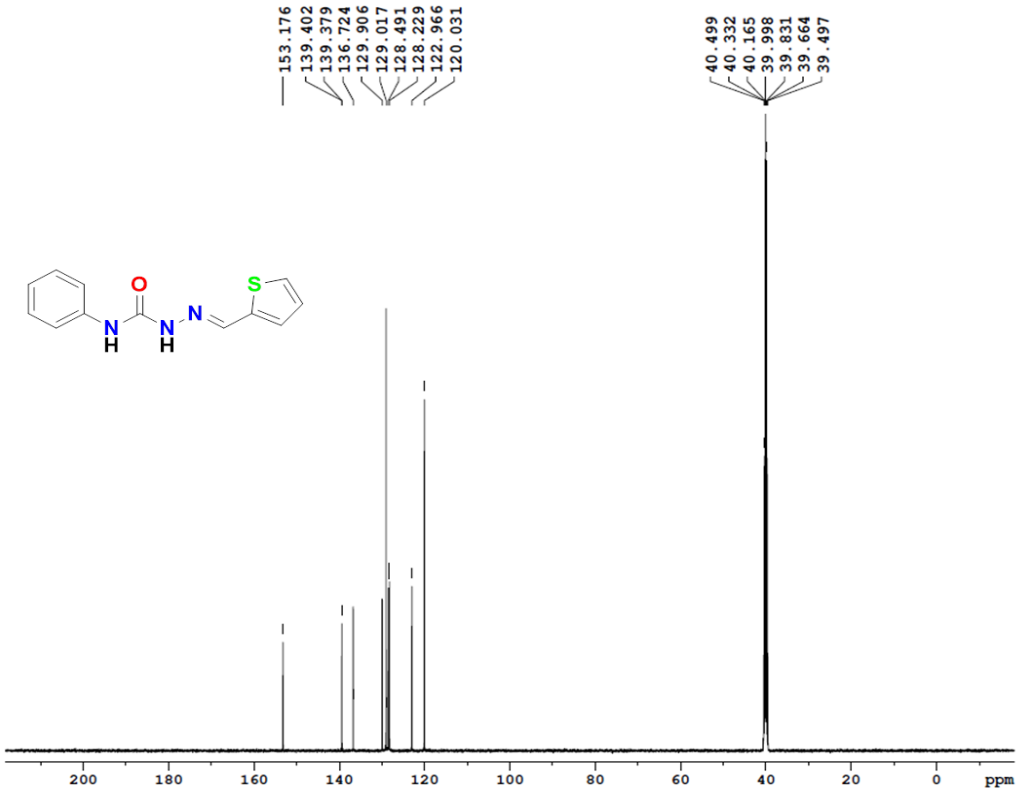

Fig. S2 — ^{13}C-NMR of synthesized Schiff base Ligand **L^{1}H**

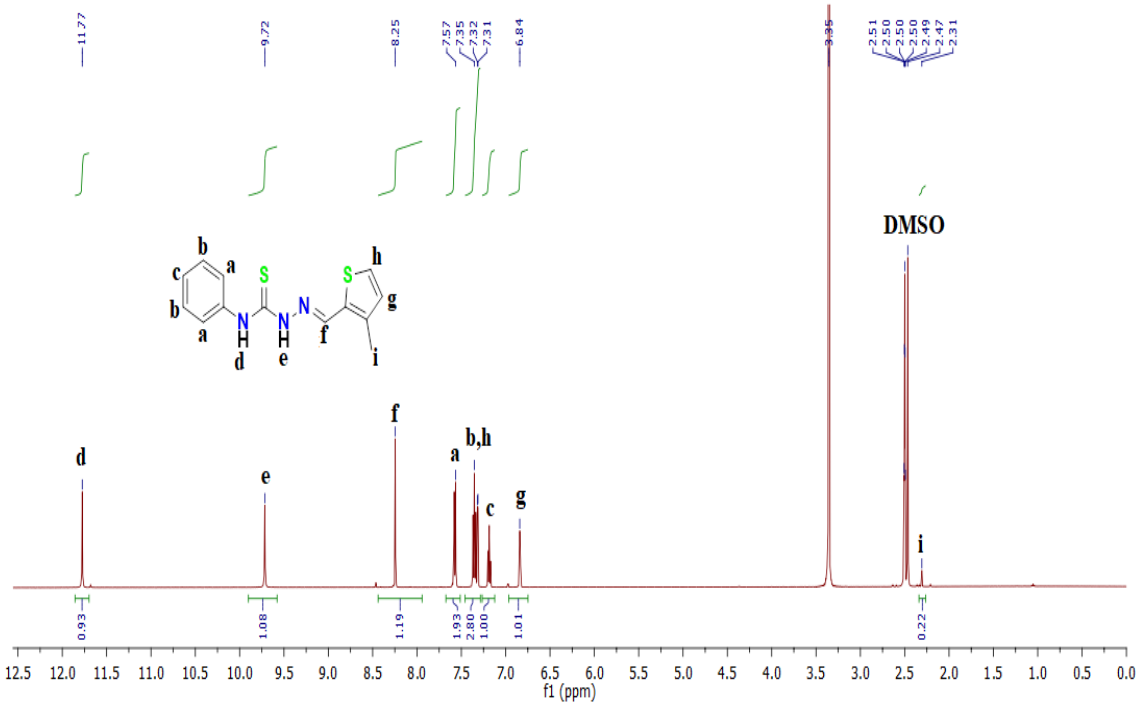

Fig. S3 — ^{1}H-NMR of synthesized Schiff base Ligand **L^{2}H**

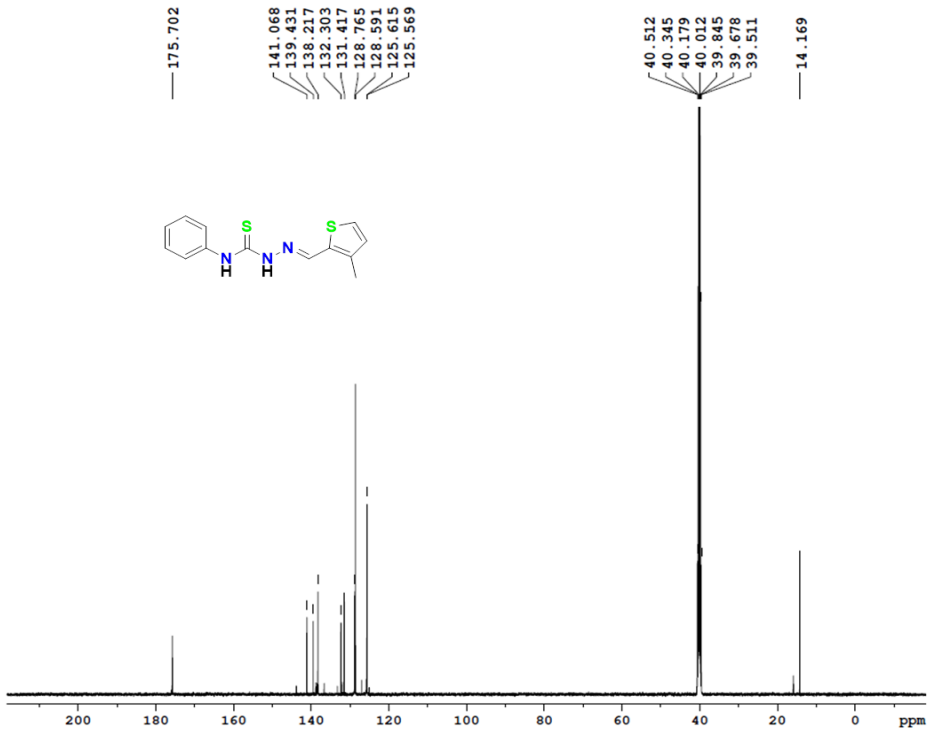

Fig. S4 — ^{13}C-NMR of synthesized Schiff base Ligand $\mathbf{L^2H}$

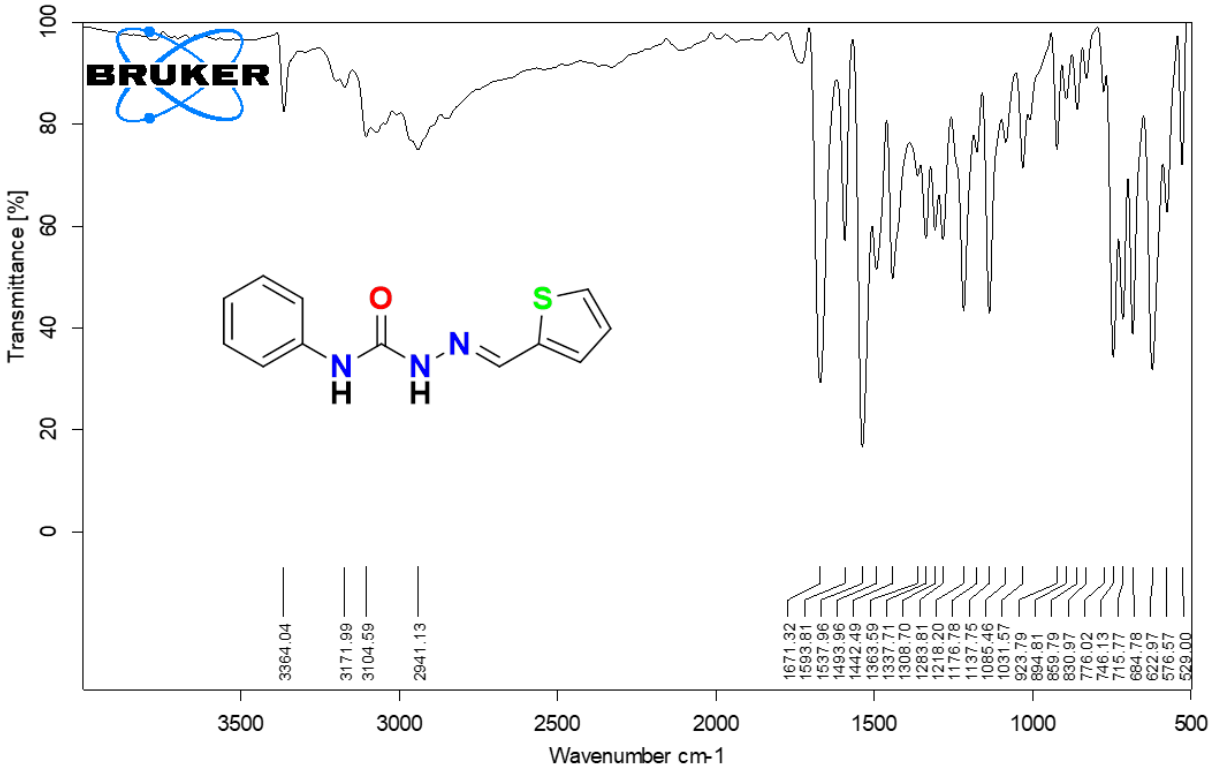

Fig. S5 — FT-IR of synthesized Schiff base Ligand $\mathbf{L^1H}$

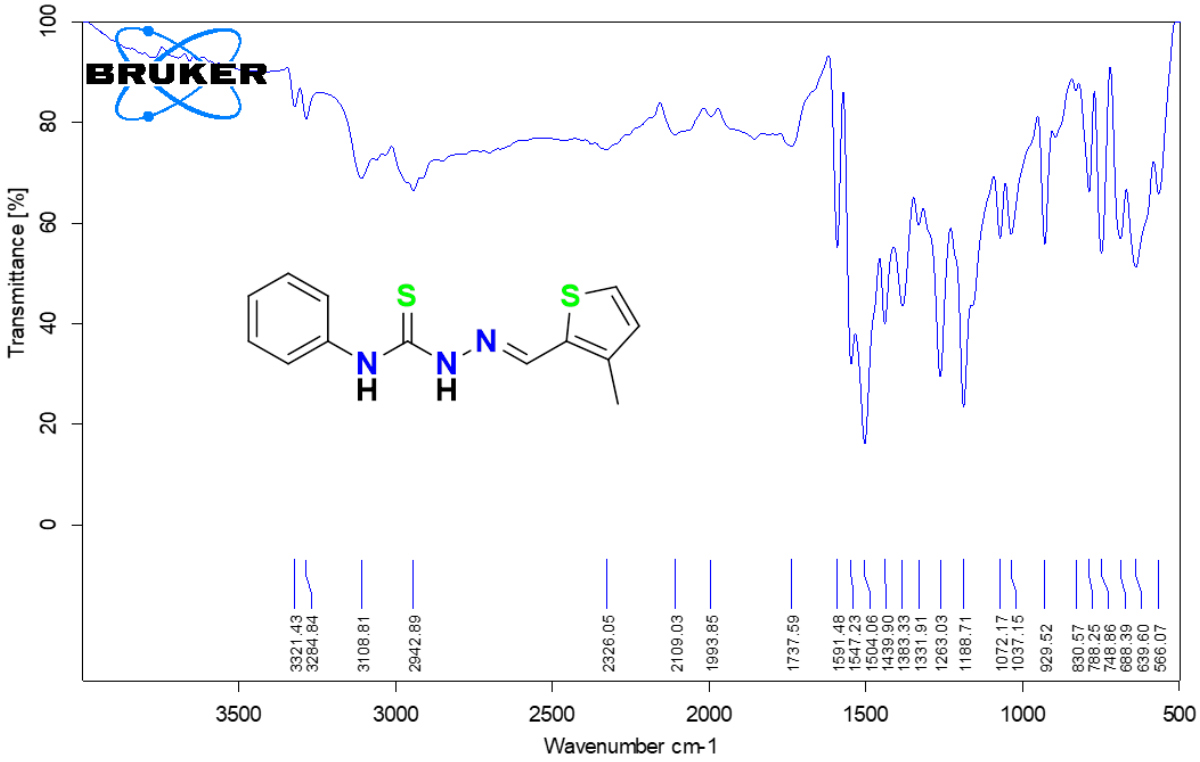

Fig. S6 — FT-IR of synthesized Schiff base Ligand $\mathbf{L^2H}$

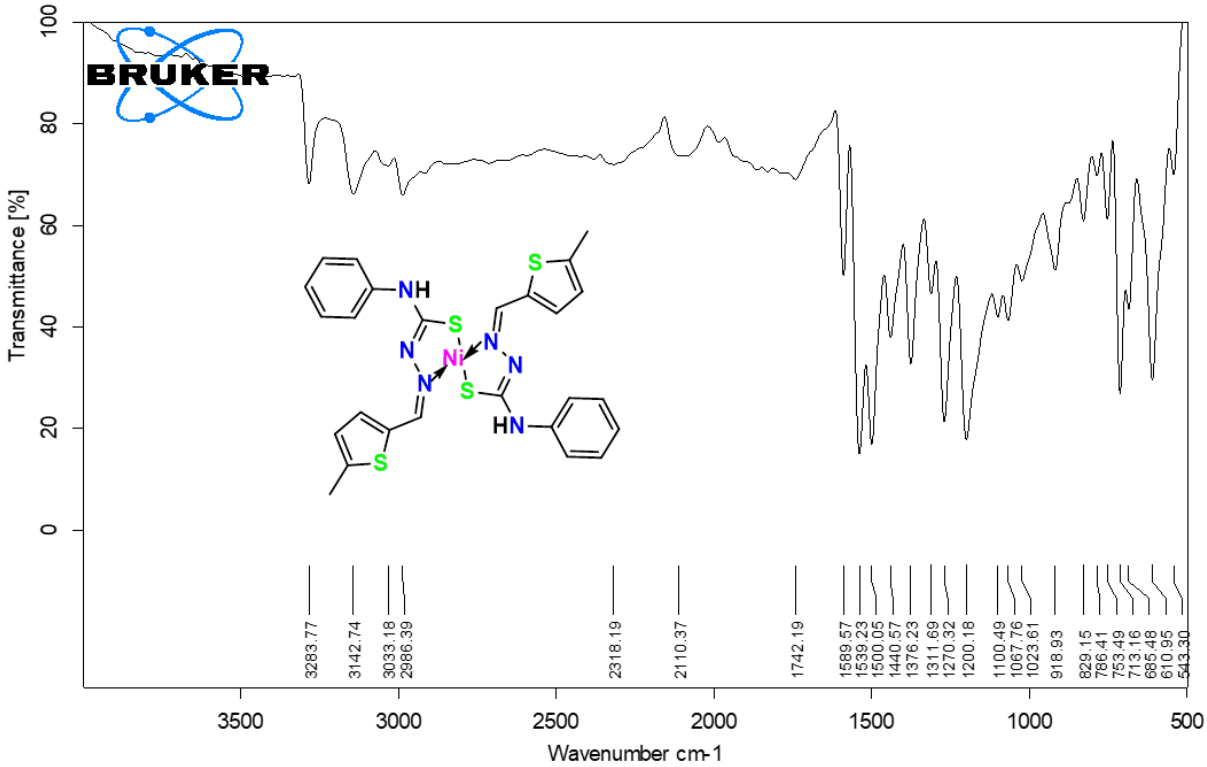

Fig. S7— FT-IR of synthesized Ni(II) complex [Ni(L^2)$_2$] **(3)**

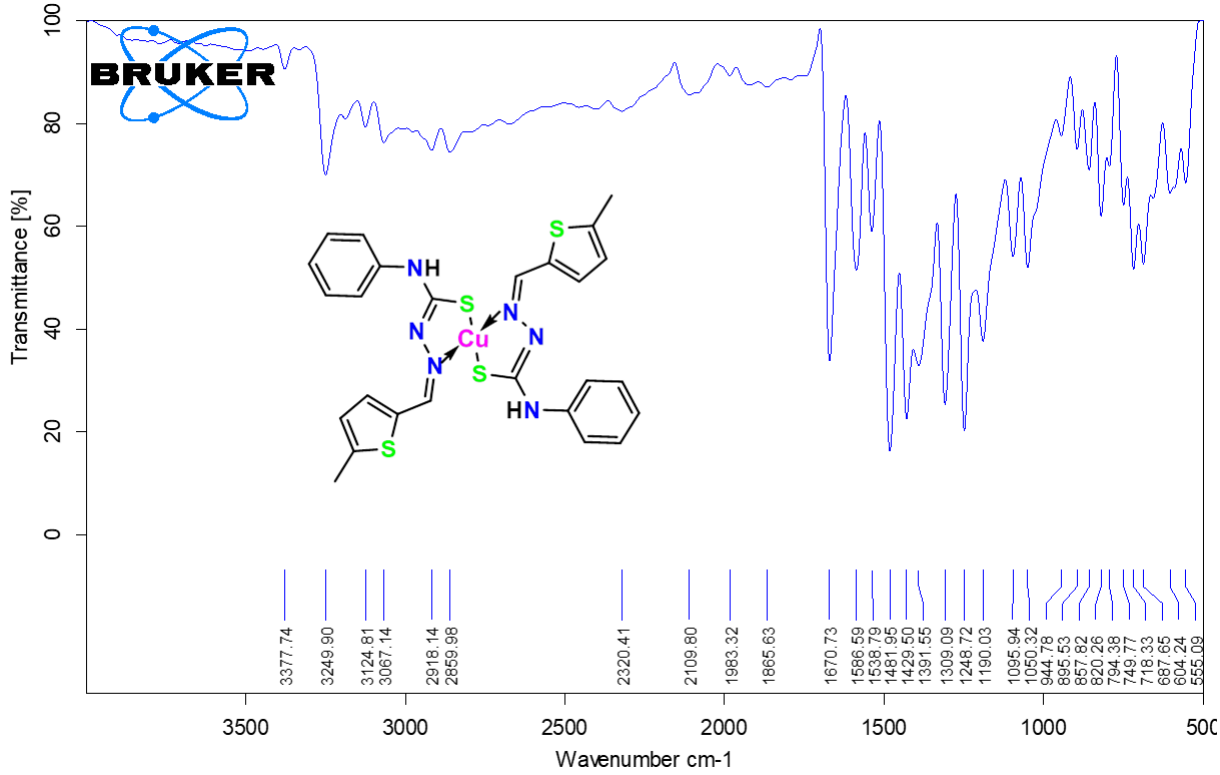

Fig. S8— FT-IR of synthesized Ni(II) complex [Cu(L^2)$_2$] **(3)**

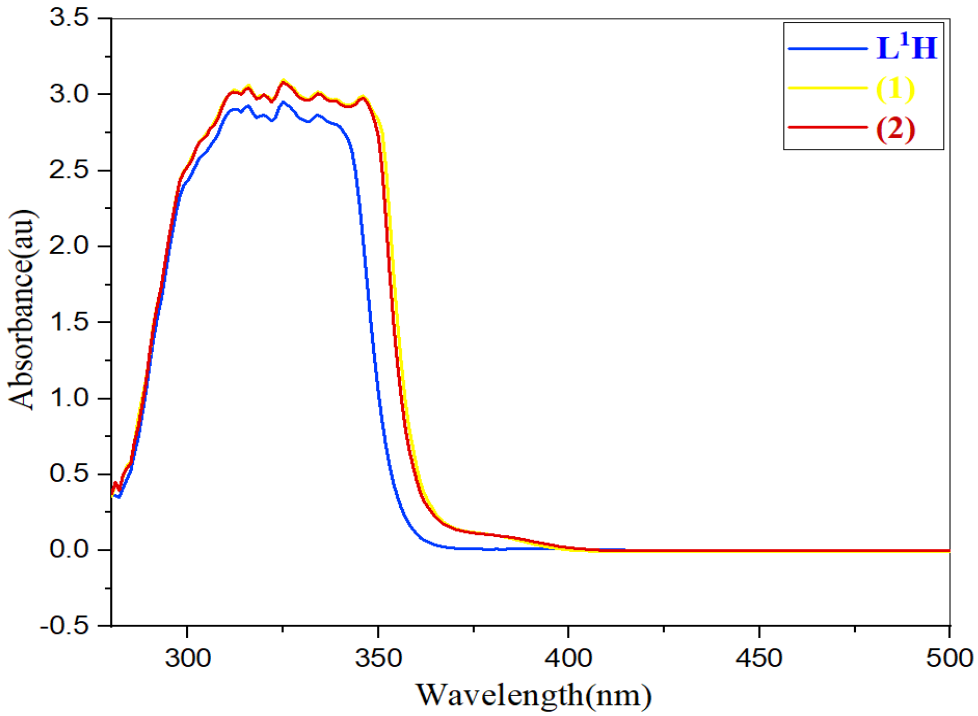

Fig. S9 — UV-visible absorption spectra of synthesized Schiff base ligand **L^1H** and its metal(II) complexes **(1)** and **(2)**

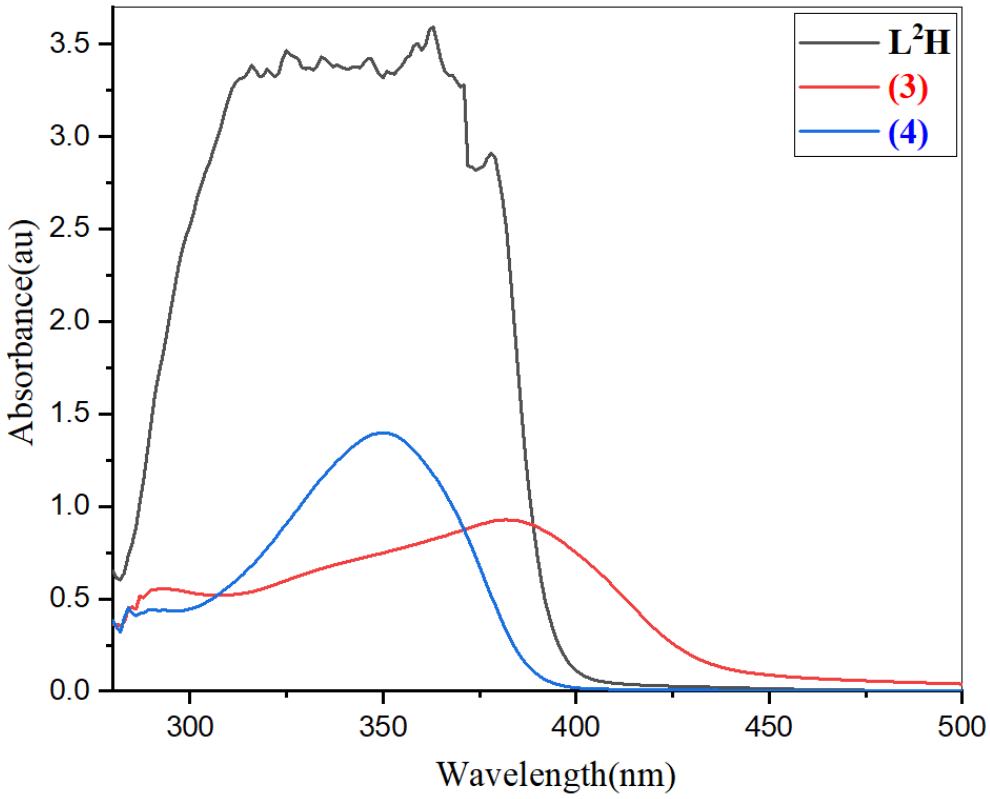

Fig. S10 — UV- visible absorption spectra of synthesized Schiff base ligand **L^2H** and its metal(II) complexes **(3)** and **(4)**

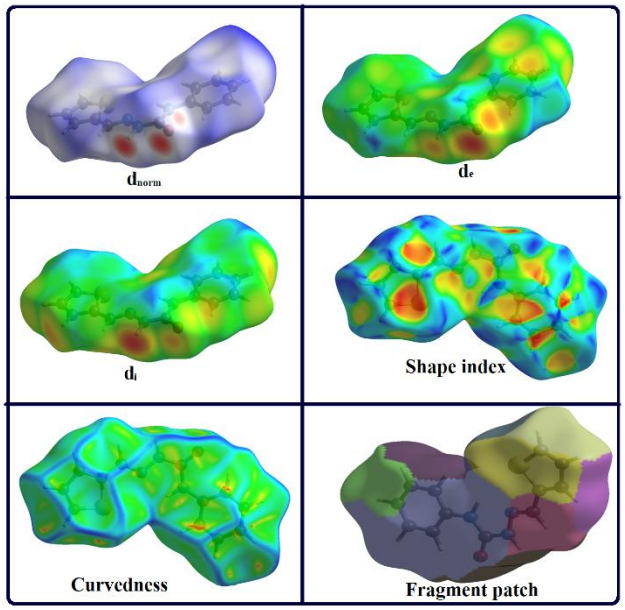

Fig. S11 — Graphical view of the Hirshfeld surfaces mapped with d_{norm} property visualizing the interaction of the Schiff base ligand **L^1H**. d_{norm} color scale in between -0.59 au (blue) and 2.07au (red). Shape index surfaces: (Red colors-Hollows, bumps-blue colors). Curvedness: (edges-blue color; flat region - green color)

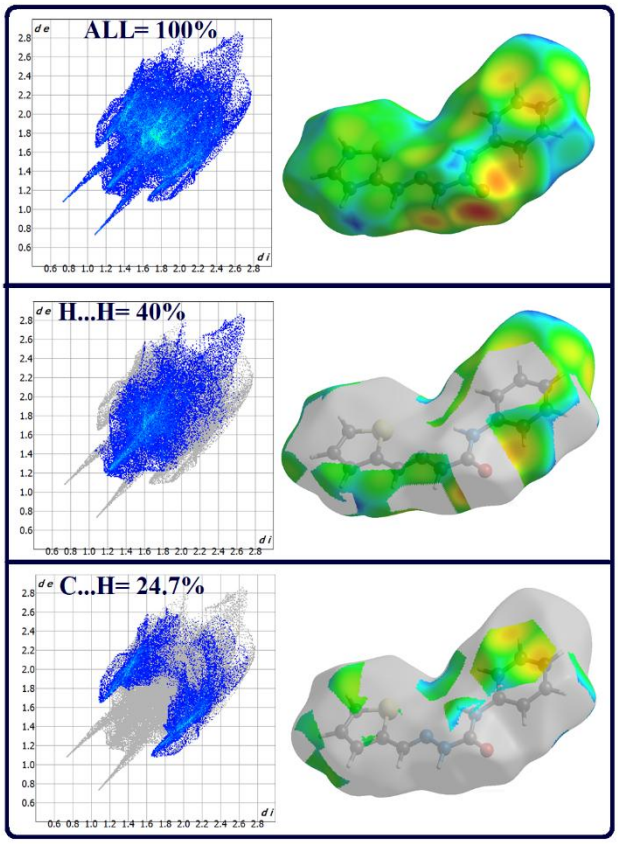

Fig. S12– Graphical view of Hirshfeld surface with 2D-fingerprint plots with characteristic features for **L^{1}H**; d_i and d_e are the distances from the surface to the nearest atoms interior and exterior to the surface respectively

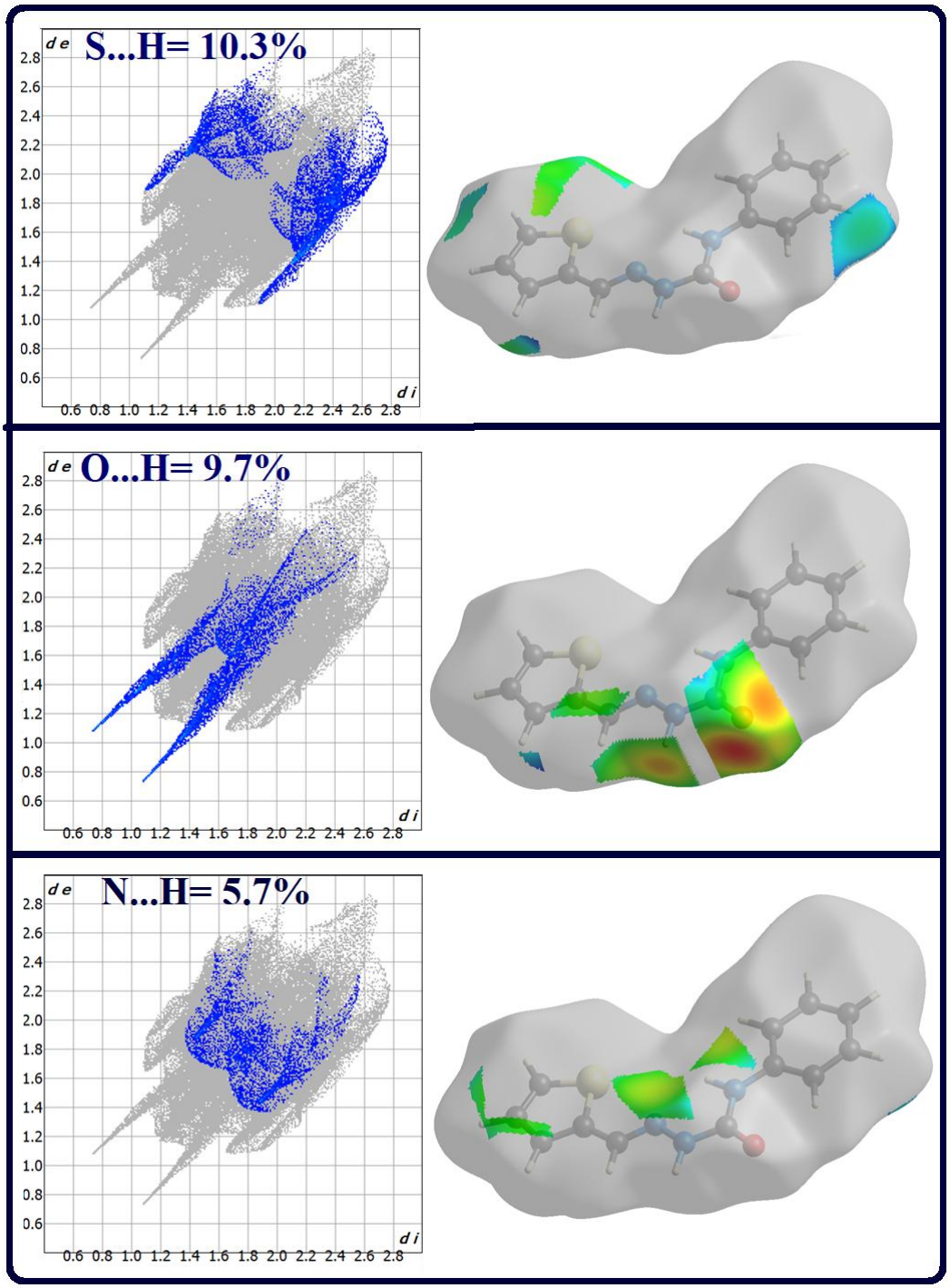

Fig. S13 ─ Graphical view of Hirshfeld surface with 2D-fingerprint plots with characteristic features for $\mathbf{L^1H}$; d_i and d_e are the distances from the surface to the nearest atoms interior and exterior to the surface respectively

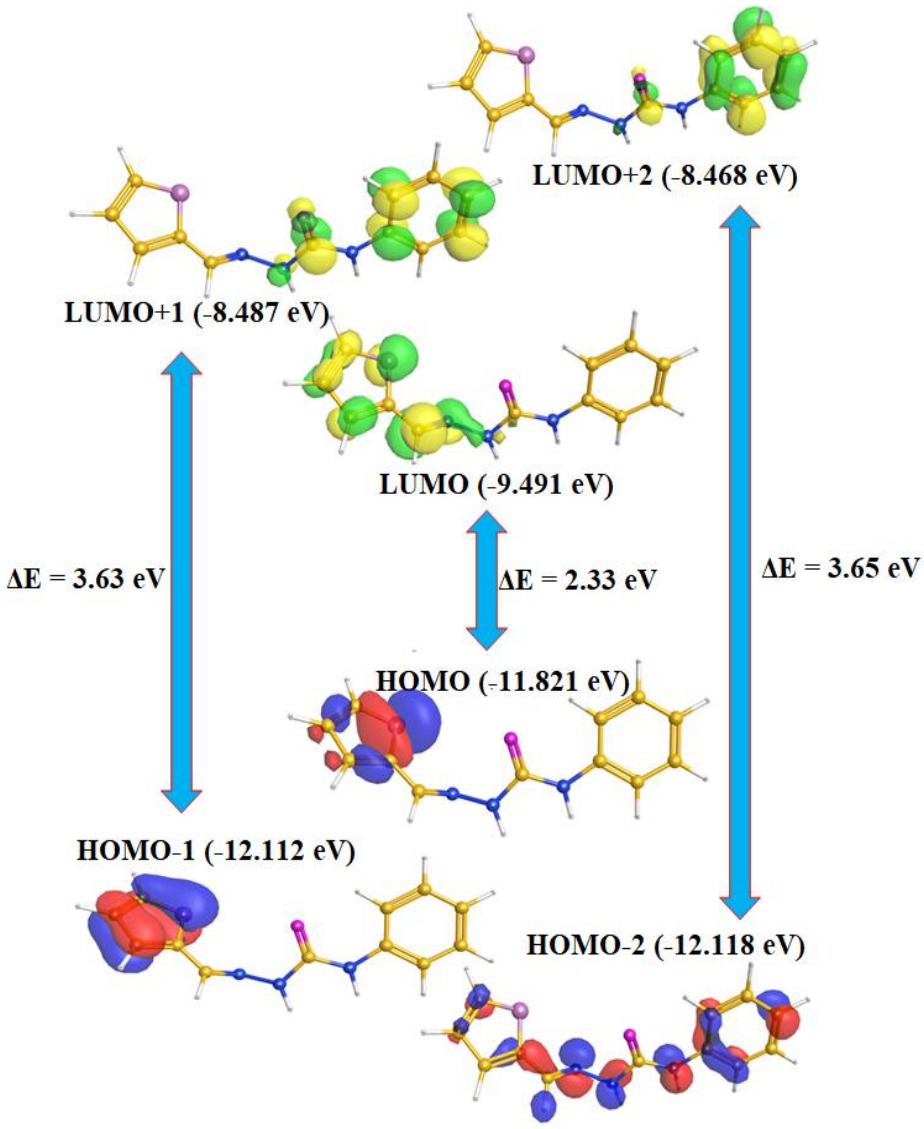

Fig. S14 — Frontier molecular orbitals diagram of Schiff base Ligand (**L^1H**)

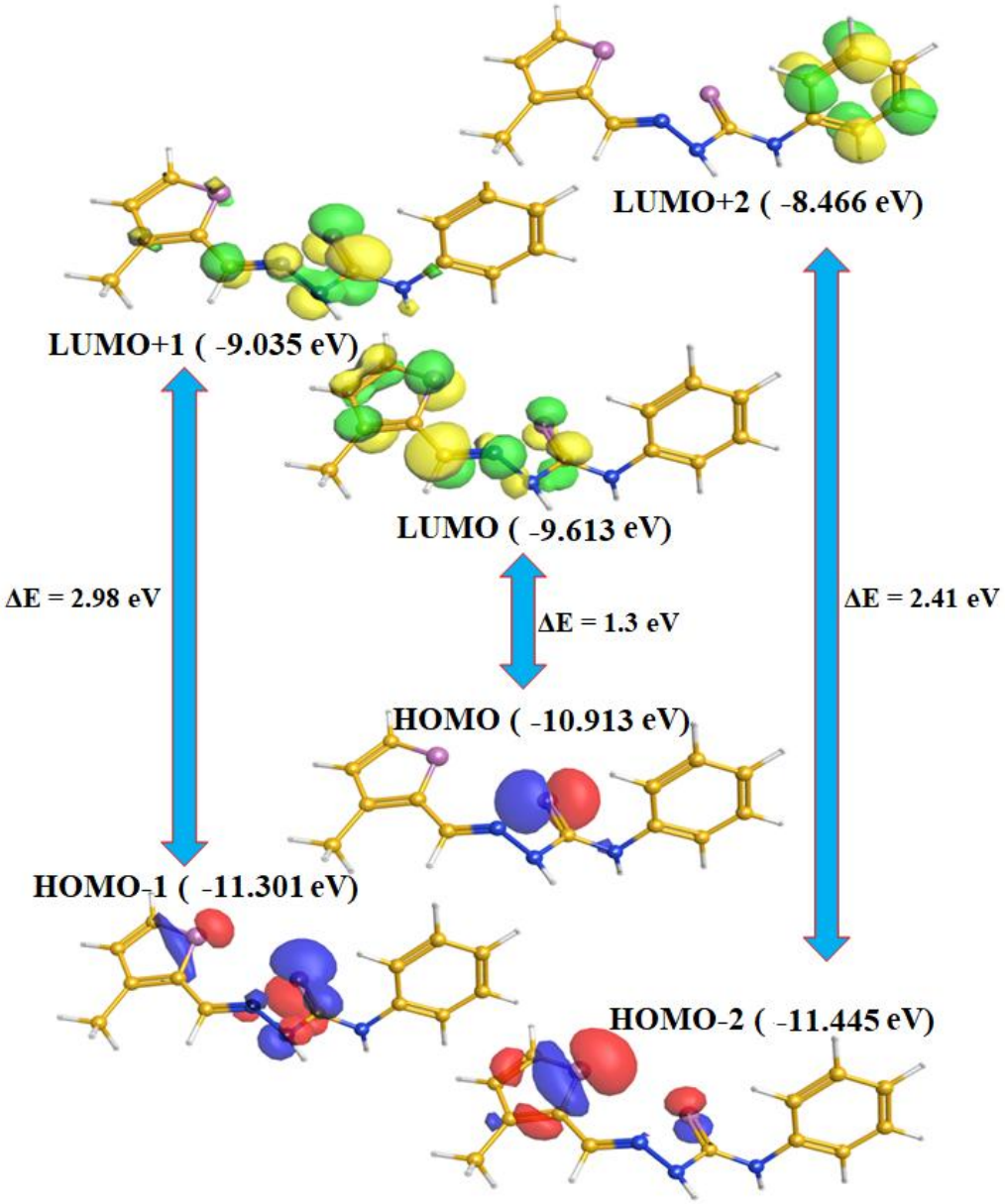

Fig. S15 — Frontier molecular orbitals diagram of Schiff base Ligand (**L^2H**)

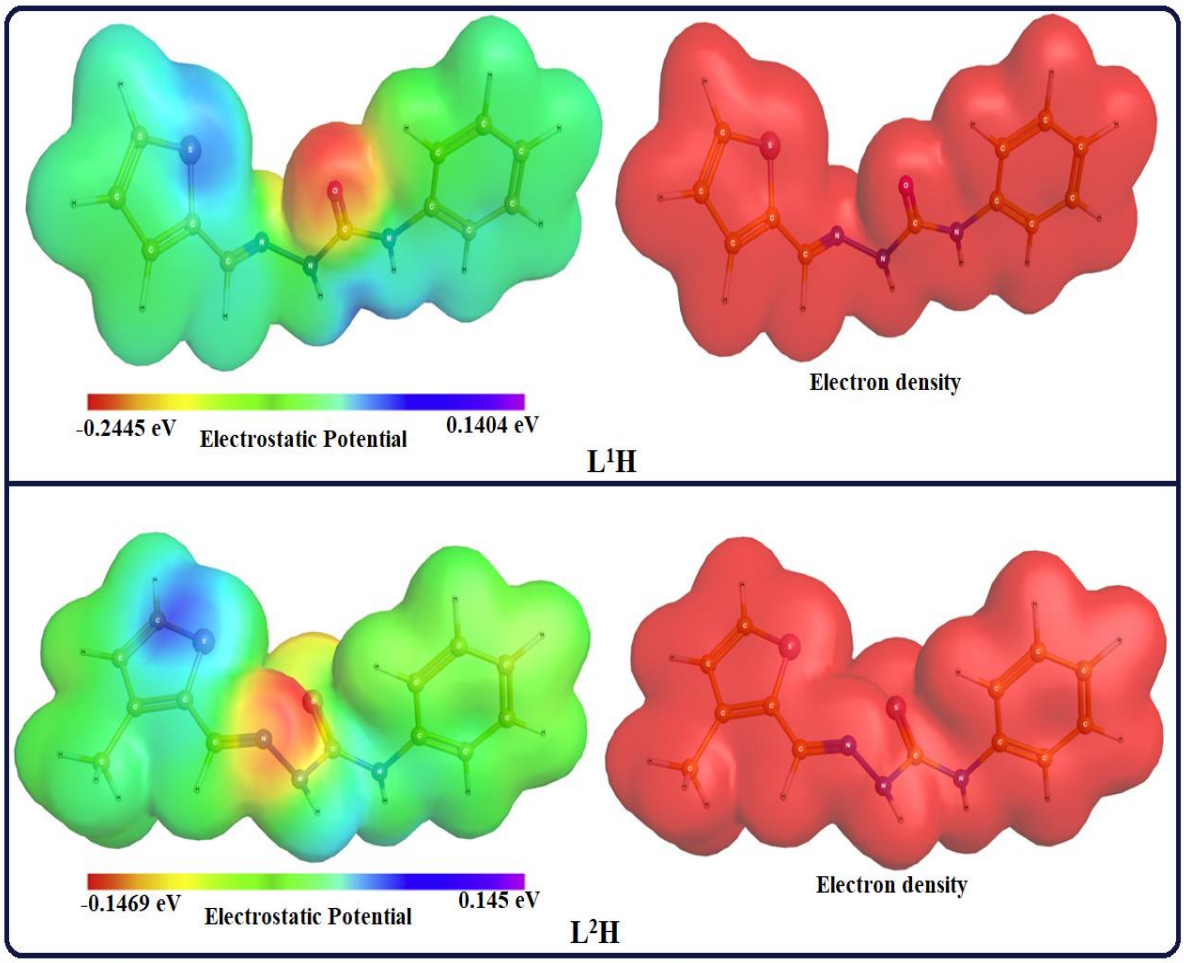

Fig. S16 ─ Molecular electrostatic potential (MEP) maps and electron density surface representation of **L^1H** and **L^2H**

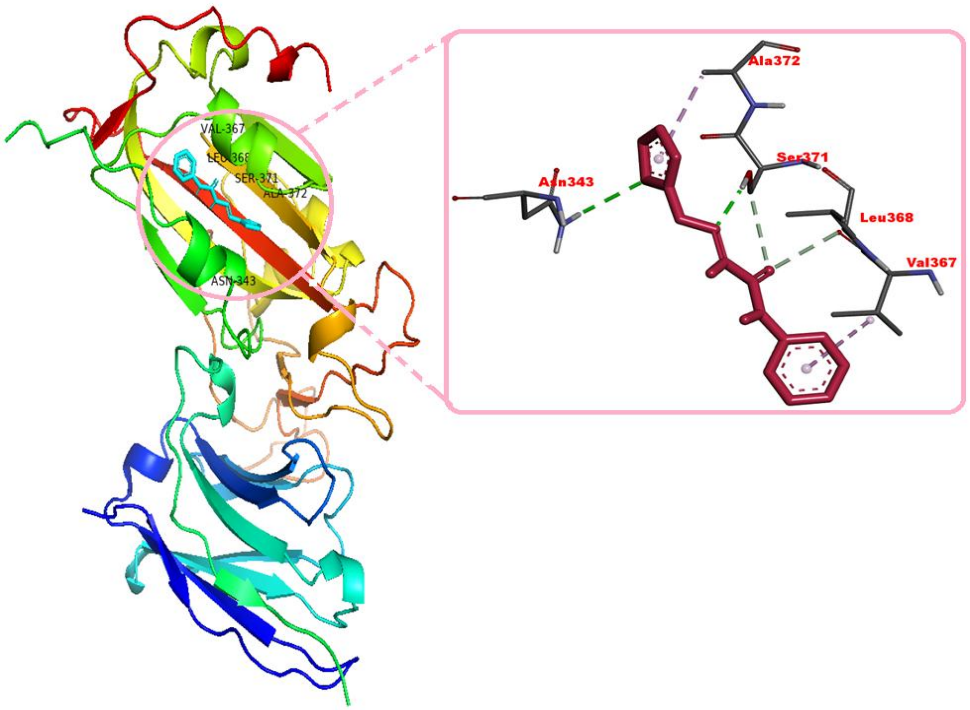

Fig. S17 — The docked Schiff base ligand **L^1H** inside the SARS-CoV M^{Pro}(7VNB) with its focused view for interacting residues around the docked complex

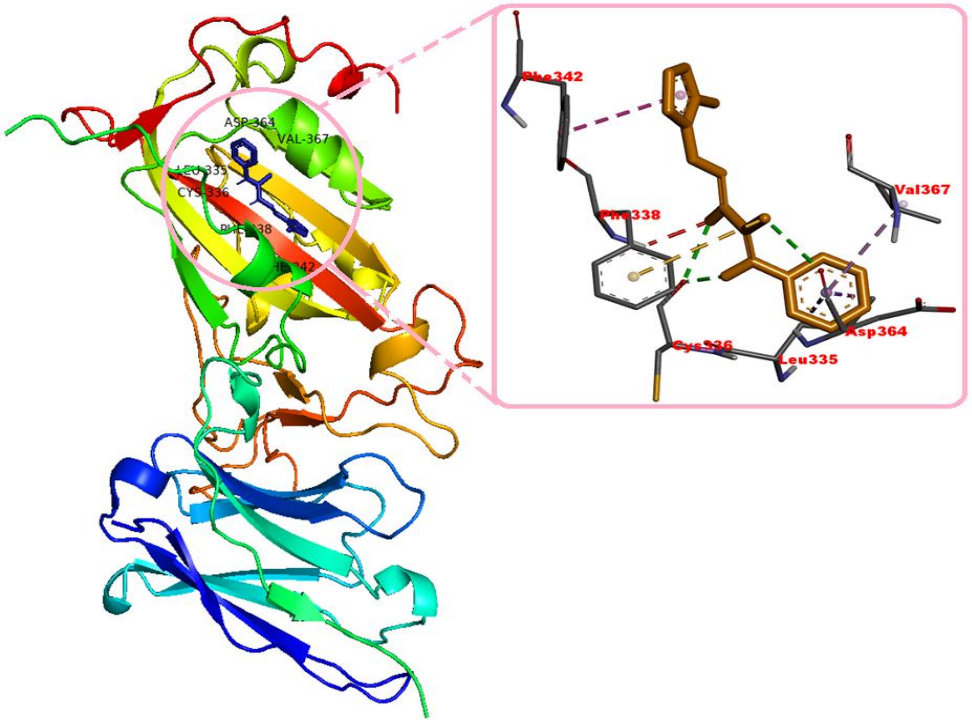

Fig. S18 — The docked Schiff base ligand **L^2H** inside the SARS-CoV M^{Pro}(7VNB) with its focused view for interacting residues around the docked complex

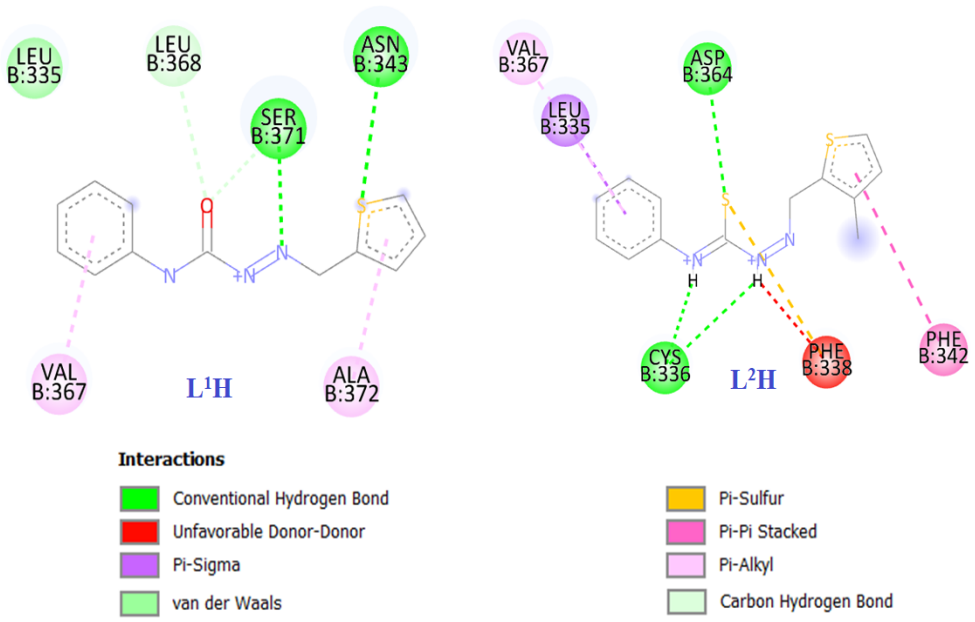

Fig. 19 ─ 2-D representation of docked Schiff bnase ligands **L^1H** and **L^2H** inside the SARS-CoV M^{Pro}(7VNB) with its focused view for interacting residues around the docked complex

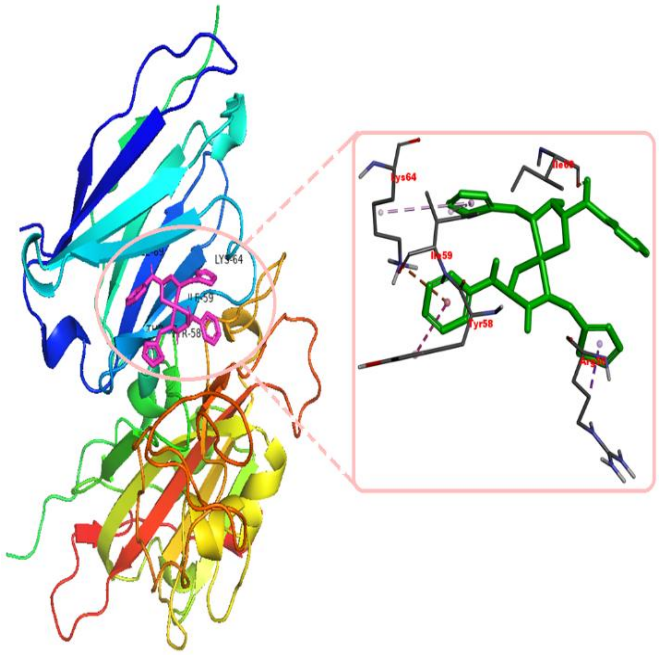

Fig. S20 ─ The docked Ni(II) complex [Ni(L^1)$_2$] **(1)** inside the SARS-CoV M^{Pro}(7VNB) with its focused view for interacting residues around the docked complex

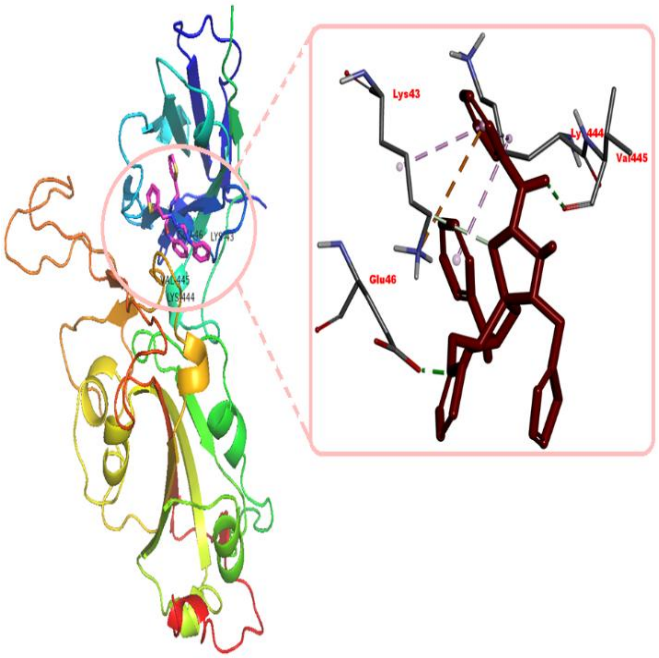

Fig. S21 ─ The docked Ni(II) complex [Cu(L^1)$_2$] **(2)** inside the SARS-CoV M^{Pro}(7VNB) with its focused view for interacting residues around the docked complex

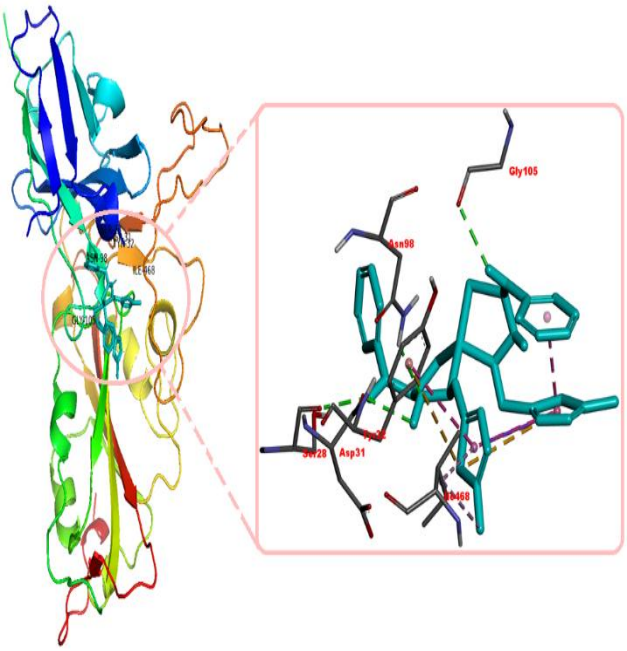

Fig. S22 ─ The docked Ni(II) complex $[Ni(L^2)_2]$ **(3)** inside the SARS-CoV M^{Pro}(7VNB) with its focused view for interacting residues around the docked complex

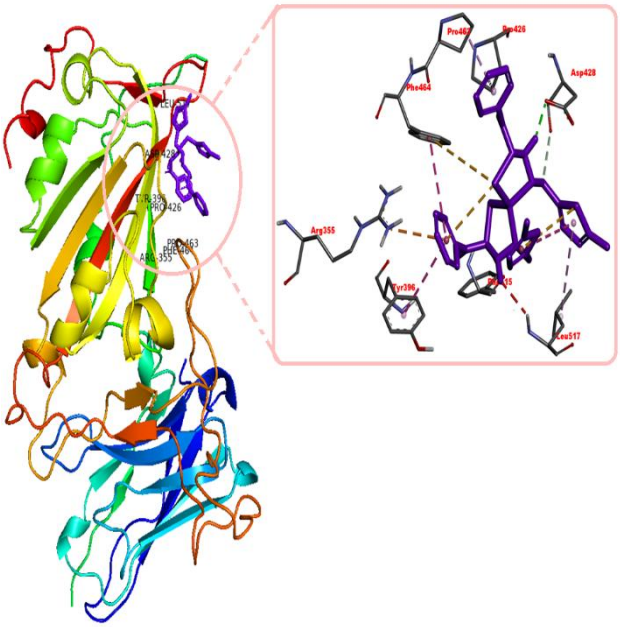

Fig. S23 ─ The docked Cu(II) complex $[Cu(L^2)_2]$ **(4)** inside the SARS-CoV M^{Pro}(7VNB) with its focused view for interacting residues around the docked complex

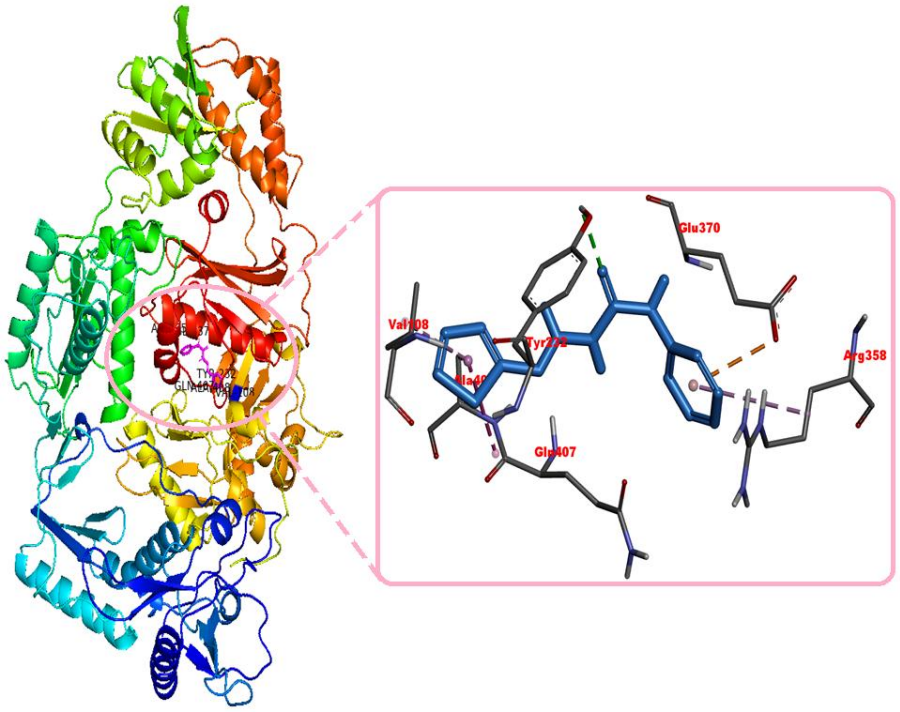

Fig. S24 — The $\mathbf{L^1H}$ inside the HIV virus (1REV) with its focused view for interacting residues around the docked complex

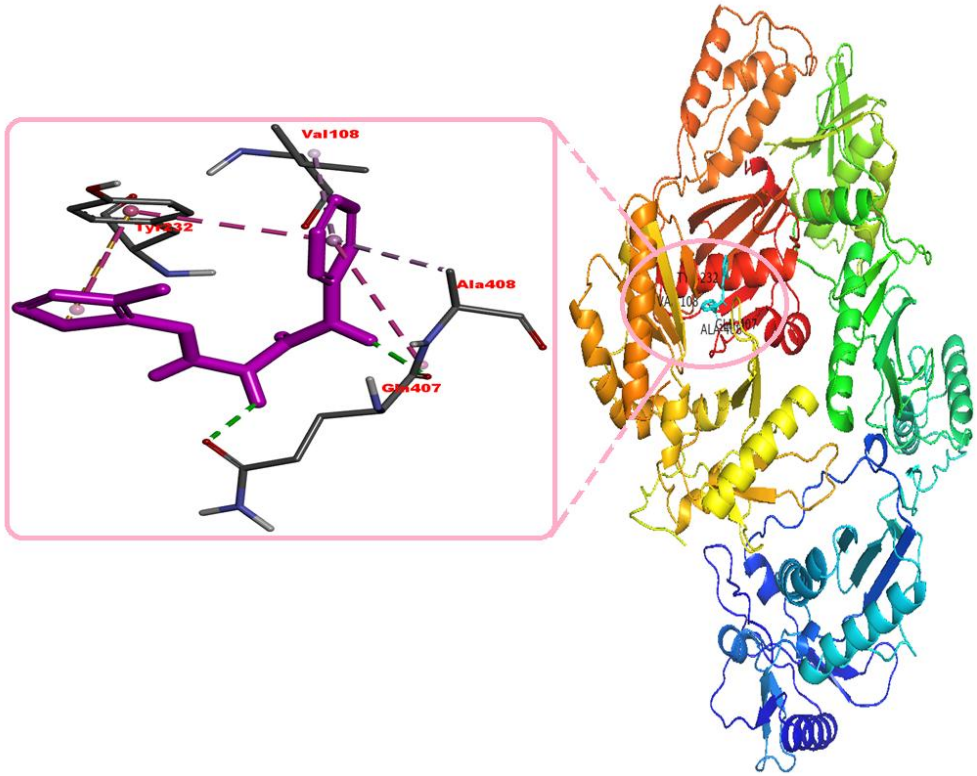

Fig. S25 — The $\mathbf{L^2H}$ inside the HIV virus (1REV) with its focused view for interacting residues around the docked complex

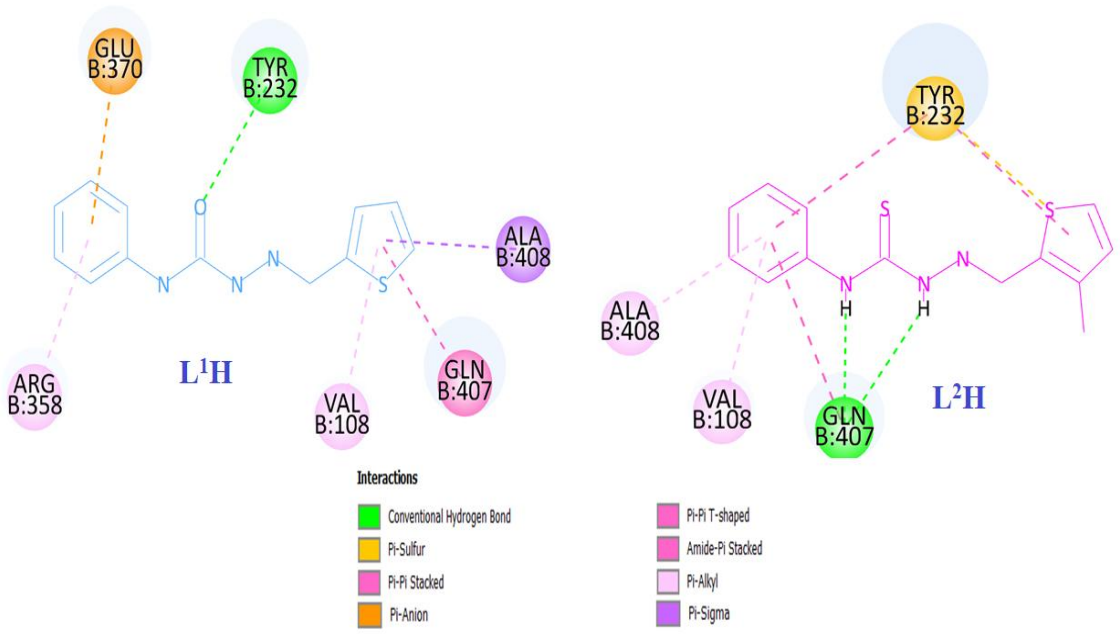

Fig. S26 ─ 2-D representation of docked Schiff bnase ligands **L^1H** and **L^2H** inside the HIV virus (1REV) with its focused view for interacting residues around the docked complex

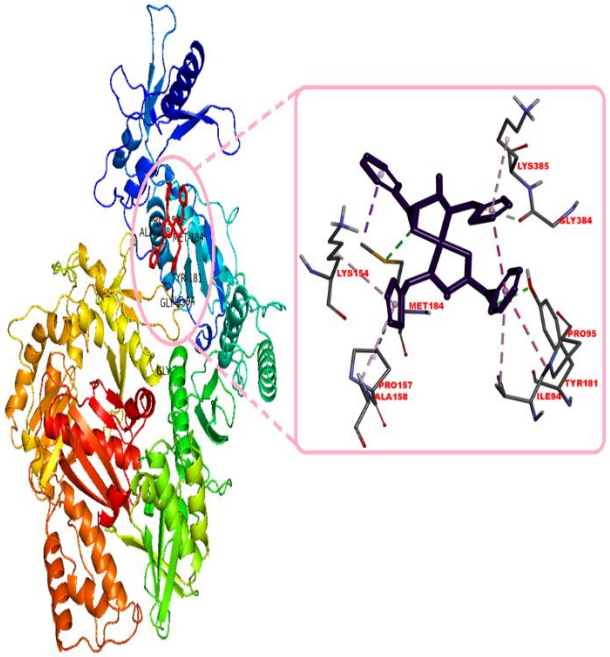

Fig. S27 ─ The Ni(II) complex $[Ni(L^1)_2]$ **(1)** inside the HIV virus (1REV) with its focused view for interacting residues around the docked complex

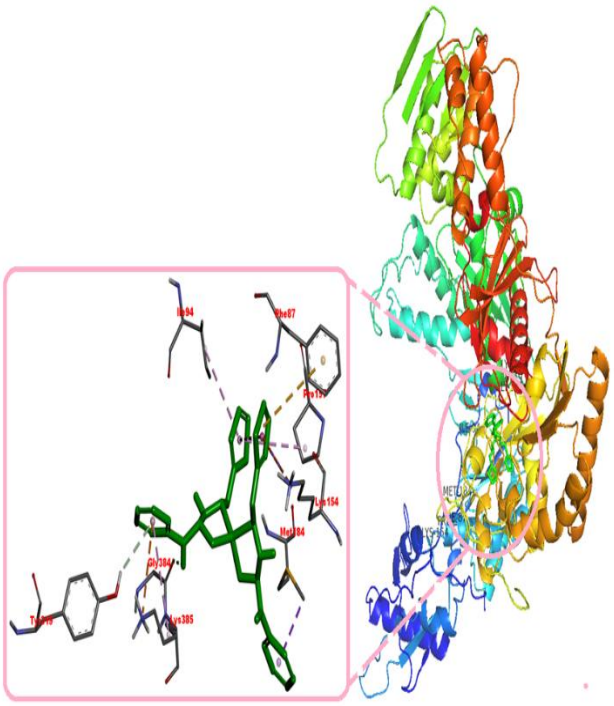

Fig. S28 ─ The Cu(II) complex $[Cu(L^1)_2]$ **(2)** inside the HIV virus (1REV) with its focused view for interacting residues around the docked complex

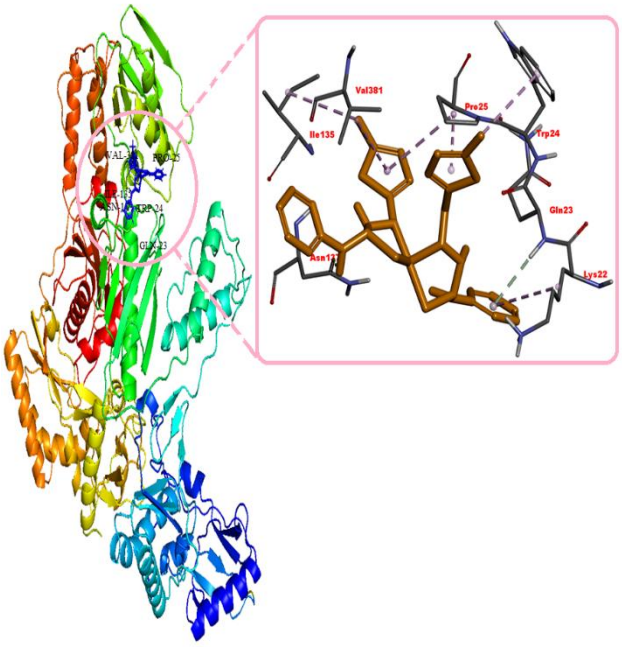

Fig. S29 ─ The Ni(II) complex $[Ni(L^1)_2]$ **(3)** inside the HIV virus (1REV) with its focused view for interacting residues around the docked complex

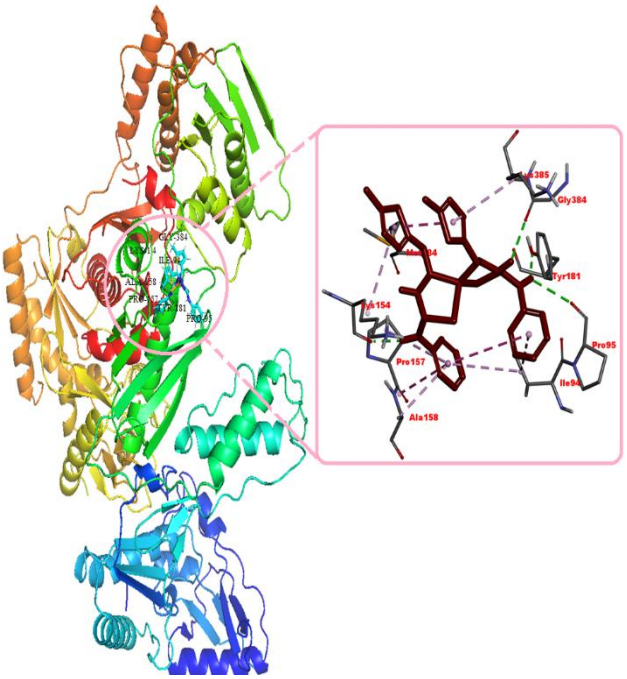

Fig. S30 ─ The Cu(II) complex [Cu(L^1)$_2$] **(4)** inside the HIV virus (1REV) with its focused view for interacting residues around the docked complex

Table S1 ─ Bond distances (Å) and bond angles (°) for Schiff base ligand (**L^1H**)			
Bond lengths (Å)			
C (6)-N (3)	1.407(3)	C (9)-S (1)	1.719(2)
C (7)-O (1)	1.236(2)	C (12)-S (1)	1.703(2)
C (7)-N (3)	1.346(3)	N (1)-N (2)	1.373(2)
C (7)-N (2)	1.362(3)	N(2)-H(2A)	0.877(15)
C (8)-N (1)	1.275(3)	N(3)-H(3A)	0.843(16)
Bond angles (°)			
C (1)-C (6)-N (3)	124.32(19)	C (5)-C (6)-N (3)	116.58(18)
O (1)-C (7)-N (3)	124.72(19)	O (1)-C (7)-N (2)	120.18(19)
N (3)-C (7)-N (2)	115.09(18)	N (1)-C (8)-C (9)	121.47(18)
N (1)-C (8)-H (8)	119.3	C (10)-C (9)-S (1)	111.09(15)
C (8)-C (9)-S (1)	122.02(15)	C (11)-C (12)-S (1)	112.88(17)
S (1)-C (12)-H (12)	123.6	C (8)-N (1)-N (2)	116.23(17)
C (7)-N (2)-N (1)	119.78(17)	C(7)-N(2)-H(2A)	121.1(14)
N(1)-N(2)-H(2A)	118.1(14)	C (7)-N (3)-C (6)	129.75(17)
C(7)-N(3)-H(3A)	113.1(16)	C(6)-N(3)-H(3A)	117.1(16)
C (12)-S (1)-C (9)	91.00(11)		

Table S2 — Interaction energies for **L[1]H** calculated with CE-B3LYP model. It can be seen from the interaction energies table that the hydrogen bonding motif between the central molecules (highlighted in yellow mesh) and the -x +1/2, y+1/2, z +1/2 symmetry-related molecule (line green) is by far the strongest interaction among near neighbors

	N	Symop	R	Electron Density	E_ele	E_pol	E_dis	E_rep	E_tot
	2	-y+1/3, x-y+2/3, z+2/3	8.82	B3LYP/6-31G(d,p)	-2.3	-0.8	-12.8	9.3	-8.4
	2	-x+y+2/3, -x+1/3, z+1/3	9.40	B3LYP/6-31G(d,p)	3.6	-1.2	-10.9	5.2	-3.4
	2	x, y, z	5.62	B3LYP/6-31G(d,p)	-6.7	-2.0	-50.1	25.8	-36.3
	1	-x+1/3, -y+2/3, -z+2/3	7.45	B3LYP/6-31G(d,p)	-101.8	-24.6	-18.7	97.9	-81.6
	1	x-y+2/3, x+1/3, -z+1/3	7.99	B3LYP/6-31G(d,p)	-3.1	-0.8	-15.4	8.2	-12.3
	1	y+2/3, -x+y+1/3, -z+1/3	7.99	B3LYP/6-31G(d,p)	-3.1	-0.8	-15.4	8.2	-12.3
	1	-x+1/3, -y+2/3, -z+2/3	8.08	B3LYP/6-31G(d,p)	-3.8	-1.6	-6.6	0.3	-10.8
	1	x-y+2/3, x+1/3, -z+1/3	7.25	B3LYP/6-31G(d,p)	-10.6	-2.6	-11.0	10.5	-16.3
	1	y+2/3, -x+y+1/3, -z+1/3	7.25	B3LYP/6-31G(d,p)	-10.6	-2.6	-11.0	10.5	-16.3

Energy Model	k_ele	k_pol	k_disp	k_rep
CE-HF ... HF/3-21G electron densities	1.019	0.651	0.901	0.811
CE-B3LYP ... B3LYP/6-31G(d,p) electron densities	1.057	0.740	0.871	0.618